

## GIANT MONOPOLE RESONANCE IN Cd AND Sn ISOTOPES\*

Y.-W. LUI<sup>a</sup>, D.H. YOUNGBLOOD<sup>a</sup>, H.L. CLARK<sup>a</sup>, Y. TOKIMOTO<sup>a</sup>  
AND B. JOHN<sup>a,b</sup>

<sup>a</sup>Cyclotron Institute, Texas A&M University, College Station  
Texas 77843, USA

<sup>b</sup>Nuclear Physics Division, Bhabha Atomic Research Center  
Mumbai-400085, India

*(Received November 30, 2004)*

The giant resonance region from  $10 \text{ MeV} < E_x < 55 \text{ MeV}$  in  $^{110}\text{Cd}$ ,  $^{116}\text{Cd}$ ,  $^{112}\text{Sn}$  and  $^{124}\text{Sn}$  has been studied with inelastic scattering of 240 MeV  $\alpha$  particles at small angles including  $0^\circ$ . Essentially, all of the E0 strength in these nuclei was located. The isotopic dependence of the giant monopole resonance energies was found to be consistent with relativistic and nonrelativistic calculations for interactions with  $K_{nm} \sim 220\text{--}240 \text{ MeV}$ . PACS numbers: 25.55.Ci, 24.30.Cz, 27.60.+j

### 1. Introduction

The locations of the isoscalar giant monopole resonance (GMR) are important because its energy can be directly related to the nuclear compressibility and from this the compressibility of nuclear matter ( $K_{nm}$ ) can be obtained [1, 2]. Of particular interest is the variation of compressibility with neutron number. Studies of the GMR in the Sn isotopes were carried out a number of years ago [3, 4] to determine the isotopic behavior of the GMR with an emphasis on determining the coefficient of the symmetry term  $((N - Z)/A)$  in the Leptodermous expansion. These data has relatively large errors compared to what is now possible. Furthermore, because of the much improved peak-to-continuum ratio [5] we can now look at the actual distribution of strength which was not possible then. With this in mind, we have studied Cd ( $^{110}\text{Cd}$ ,  $^{116}\text{Cd}$ ) and Sn ( $^{112}\text{Sn}$ ,  $^{124}\text{Sn}$ ) isotopes with small-angle inelastic  $\alpha$  scattering at 240 MeV, which has been very useful in obtaining strength distributions of isoscalar electric multipoles in several nuclei [5].

---

\* Presented at the XXXIX Zakopane School of Physics — International Symposium “Atomic Nuclei at Extreme Values of Temperature, Spin and Isospin”, Zakopane, Poland, August 31–September 5, 2004.

## 2. Experimental technique and data analysis

The experimental technique has been described thoroughly in Ref. [5] and is summarized briefly below. Beams of 240 MeV  $\alpha$  particles from the Texas A&M K500 superconducting cyclotron bombarded self supporting foils located in the target chamber of the multipole-dipole-multipole spectrometer. The horizontal acceptance of the spectrometer was  $4^\circ$  and ray tracing was used to reconstruct the scattering angle. The vertical acceptance was set at  $\pm 2^\circ$ . The focal plane detector measured position and angle in the scattering plane and covered from 47 to 55 MeV of excitation, depending on scattering angle. The out-of-plane scattering angle was not measured. Position resolution of approximately 0.9 mm and scattering angle resolution of about  $0.09^\circ$  were obtained. At  $\theta_{\text{spec}} = 0^\circ$ , runs with an empty target frame had an  $\alpha$ -particle rate approximately 1/2000 of that with a target in place, and  $\alpha$  particles were uniformly distributed in the spectrum. Cross sections were obtained from the charge collected, target thickness, dead time, and known solid angle. The target thickness were measured by weighing and checked by measuring the energy loss of the 240 MeV  $\alpha$  beam in each target. The

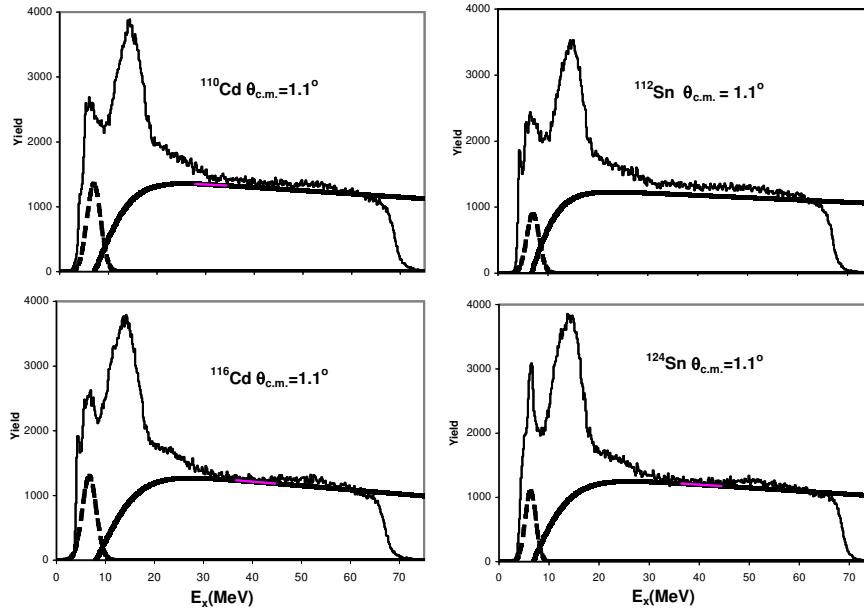


Fig. 1. Inelastic  $\alpha$  spectra obtained for  $^{110}\text{Cd}$ ,  $^{116}\text{Cd}$ ,  $^{112}\text{Sn}$  and  $^{124}\text{Sn}$ . The thick lines show the continuum chosen for the analysis. The dashed line below 10 MeV represents a contaminant peak present at some angles in the spectra taken with the spectrometer at  $0^\circ$ . This was subtracted before the multipole analysis was done.

cumulative uncertainties in target thickness, solid angle, *etc.*, result in about  $\pm 10\%$  in absolute cross sections.  $^{24}\text{Mg}$  spectra were taken before and after each run with each target and the  $13.85 \pm 0.02$  MeV  $L = 0$  state [6] was used as a check on calibration in the giant resonance region. Sample spectra obtained for  $^{110}\text{Cd}$ ,  $^{116}\text{Cd}$ ,  $^{112}\text{Sn}$  and  $^{124}\text{Sn}$  are shown in Fig. 1. The giant resonance peak can be seen extending up past  $E_x = 30$  MeV. The spectrum was divided into a peak and a continuum, where the continuum was assumed to have the shape of a straight line at high excitation joining onto a Fermi shape at low excitation to model particle threshold effects [5]. Samples of the continua used are also shown in Fig. 1.

### 3. Multipole analysis

The multipole components of the giant resonance peak were obtained [5] by dividing the peak into multiple regions (bins) by excitation energy and then comparing the angular distributions obtained for each of these bins to distorted wave Born approximation (DWBA) calculations. The uncertainty from the multipole fits were determined for each multipole by incrementing (or decrementing) that strength, then adjusting the strengths of the other multipoles to minimize total  $\chi^2$ . This continued until the new  $\chi^2$  was one unit larger than the total  $\chi^2$  obtained for the best fit.

Elastic scattering data were not available for these nuclei, so optical model parameters obtained for  $^{116}\text{Sn}$  [7] were used. Single folding density dependent DWBA calculations (as described in Refs. [5, 7, 8]) were carried out with Fermi mass distributions for  $^{110}\text{Cd}$ ,  $^{116}\text{Cd}$ ,  $^{112}\text{Sn}$  and  $^{124}\text{Sn}$  using  $c = 5.3435$ ,  $5.4164$ ,  $5.3714$  and  $5.4907$  fm, respectively and  $a = 0.523$  fm for all four nuclei [9]. The transition densities, sum rules, and DWBA calculations were discussed thoroughly in Ref. [5] and, except for the isoscalar dipole, the same expressions and techniques were used in this work. The transition density for inelastic  $\alpha$  particle excitation of the isoscalar giant dipole resonance given by Harakeh and Dieperink is for one magnetic substate, so that the transition density given in Ref. [10] must be multiplied by the  $\sqrt{3}$  in the DWBA calculation.

Fits to the angular distributions were carried out with a sum of isoscalar  $0^+$ ,  $1^-$ ,  $2^+$ ,  $3^-$ , and  $4^+$  strengths. The isovector giant dipole resonance contributions were calculated from the known distribution [11] and held fixed in the fits. The continuum distributions are similar over the entire energy range, whereas the angular distributions of the cross sections for the peak change as the contributions of different multipoles dominate in different energy regions.

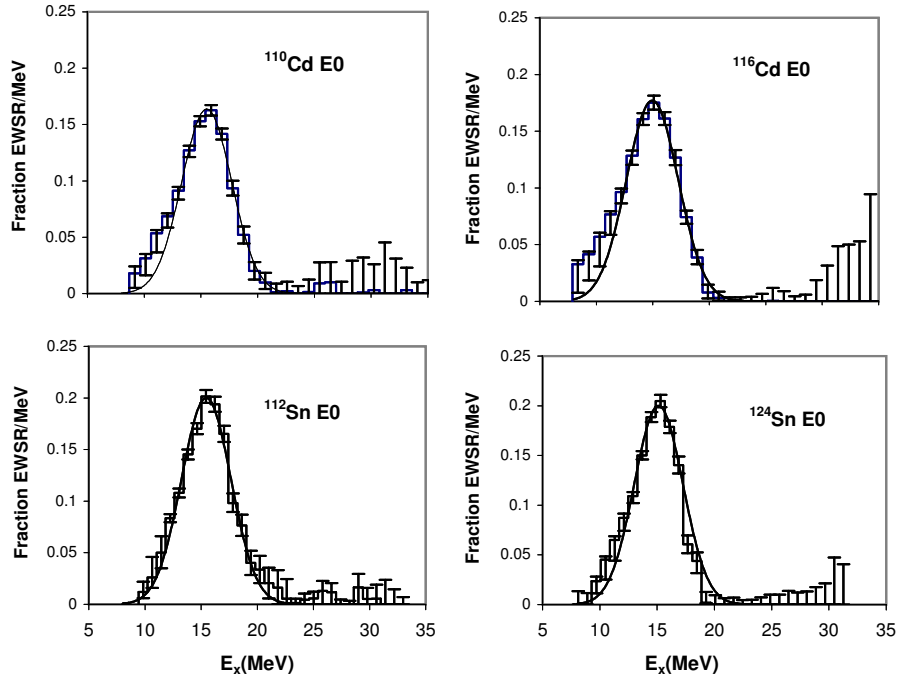


Fig. 2. E0 strength distribution obtained for  $^{110}\text{Cd}$ ,  $^{116}\text{Cd}$ ,  $^{112}\text{Sn}$  and  $^{124}\text{Sn}$  are shown by the histograms. Error bar represent the uncertainty due to the fitting of the angular distributions and different choices of the continuum, as described in the text. The smooth line show Gaussian fits.

Several analyses were carried out to assess the effects of different choices of the continuum on the resulting multipole distributions, as described in Ref. [12] where the continuum was systematically varied and the data reanalyzed. The strength distributions obtained from these analyses and from those obtained with the continua shown in the figures were then averaged, and errors calculated by adding the errors obtained from the multipole fits in quadrature to the standard deviations between the different fits. The E0 distribution for  $^{110}\text{Cd}$ ,  $^{116}\text{Cd}$ ,  $^{112}\text{Sn}$  and  $^{124}\text{Sn}$  are shown in Fig. 2 and the energy moments and sum-rule strengths obtained are summarized in Table I. Single Gaussians were fitted to the E0 distributions and are also shown in Fig. 2 and the parameters obtained are also listed in Table I.

TABLE I

Parameters obtained for E0 strength in  $^{110}\text{Cd}$ ,  $^{116}\text{Cd}$ ,  $^{112}\text{Sn}$  and  $^{124}\text{Sn}$ 

A	Moment			Gaussian Fits		Frac EWSR
	$\sqrt{m_3/m_1}$ (MeV)	rms width (MeV)	$m_1$	Centroid (MeV)	FWHM (MeV)	
$^{110}\text{Cd}$	$15.58^{+0.40}_{-0.09}$	$2.16^{+0.12}_{-0.08}$	$0.88^{+0.21}_{-0.13}$	$15.71^{+0.11}_{-0.11}$	$5.18^{+0.16}_{-0.17}$	$0.86^{+0.10}_{-0.10}$
$^{116}\text{Cd}$	$15.02^{+0.37}_{-0.12}$	$2.26^{+0.12}_{-0.10}$	$1.04^{+0.23}_{-0.13}$	$15.17^{+0.12}_{-0.11}$	$5.40^{+0.16}_{-0.14}$	$1.00^{+0.11}_{-0.11}$
$^{112}\text{Sn}$	$16.05^{+0.26}_{-0.14}$	$2.57^{+0.46}_{-0.19}$	$1.16^{+0.13}_{-0.18}$	$15.67^{+0.11}_{-0.11}$	$5.18^{+0.40}_{-0.04}$	$1.10^{+0.15}_{-0.12}$
$^{124}\text{Sn}$	$14.96^{+0.10}_{-0.11}$	$2.09^{+0.13}_{-0.09}$	$1.04^{+0.11}_{-0.11}$	$15.34^{+0.13}_{-0.13}$	$5.00^{+0.53}_{-0.03}$	$1.06^{+0.10}_{-0.20}$

#### 4. Discussion

Strength consistent with 100% of the E0 energy-weighted sum rule (EWSR) was located for all four nuclei, concentrated in an almost Gaussian peak but with some tailing at low excitation. The uncertainties in the region around  $E_x = 10$  MeV are larger than at higher excitation due to a rapidly varying solid angle near the low energy cut off in the detector and the uncertainty caused by the presence of some real background in this region (seen as a dashed peak in Fig. 1). The only previous measurements of giant resonance (GR) strength in the Cd isotopes was by Buenerd [13], who used inelastic  $^3\text{He}$  scattering at small angles and fit the data with two Gaussians, one for E0 and one for E2. However, it was concluded later that their analysis of  $^3\text{He}$  scattering did not identify all the E0 strength [14], so that a direct comparison of their energies to our results would not be meaningful. Previous measurements of E0 GR strength in  $^{112}\text{Sn}$  and  $^{124}\text{Sn}$  were reported by Youngblood *et al.* and Lui *et al.* [4], as well as Sharma *et al.* [3], using inelastic  $\alpha$  scattering. Their analyses assumed the peaks were Gaussian in shape. The Gaussian centroids we obtained agree within the errors with those obtained previously for the E0 distributions, though the widths we obtain are somewhat larger.

There are no specific calculations for E0 strength in these nuclei, however, Nayak *et al.* [15] have carried out Hartree–Fock random phase approximation calculations with several Skyrme or Skyrme-like interactions and parameterized the results in terms of the Leptodermous expansion. Farine, Pearson, and Tondeur [16] carried out a study using modified Skyrme interaction (parameterized with the Leptodermous expansion) designed to explore how the effective  $K_{nm}$  for an interaction might be changed while still providing GMR energies consistent with experimental results. Chossy and Stocker [17] have

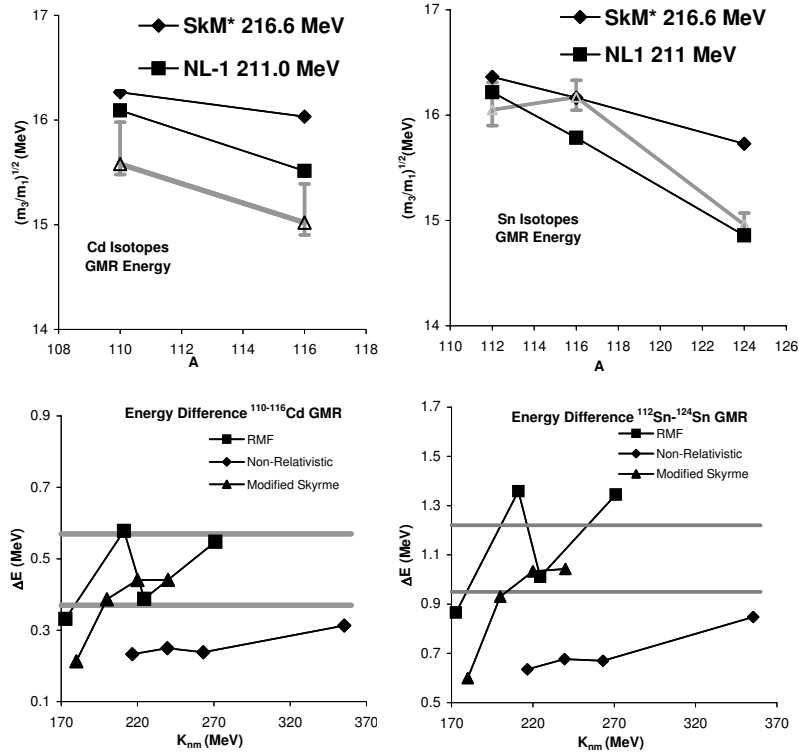


Fig. 3. Top panels: GMR energies calculated with the relativistic mean-field parameterization [17] and nonrelativistic parameterizations [15] are compared to the experimental energies shown in gray. The error bars include systematic errors. (Bottom panels: The difference in GMR energies ( $\sqrt{m_3/m_1}$ ) between  $^{110}\text{Cd}$  and  $^{116}\text{Cd}$  and between  $^{112}\text{Sn}$  and  $^{124}\text{Sn}$  calculated with the relativistic mean-field parameterization [17], nonrelativistic parameterization [15], and modified Skyrme [16] are compared to the experimental difference whose limits are indicated by the horizontal gray lines. The experimental range shown includes statistical errors, but not systematic errors.

carried out a similar parameterization for several relativistic parameter sets. E0 energies calculated with relativistic and nonrelativistic interactions are compared to the experimental energies ( $\sqrt{m_3/m_1}$ ) for the Cd isotopes in the left top panel of Fig. 3 and for Sn isotopes in the right top panel of Fig. 3. The  $^{116}\text{Sn}$  result shown in Fig. 3 was obtained from data taken along with the data for  $^{112}\text{Sn}$  and  $^{124}\text{Sn}$ , and is in excellent agreement with that reported in Ref. [18], obtained in different experimental runs. The

GMR energies in  $^{112}\text{Sn}$  and  $^{124}\text{Sn}$  appear to be low compared to  $^{116}\text{Sn}$ . The experimental energies for these nuclei are slightly below energies obtained with calculations for interactions for which  $K_{nm} \sim 211\text{--}216$  MeV. This is somewhat lower than  $K_{nm} \sim 231$  MeV, suggested by energies for a number of other nuclei [18] including  $^{116}\text{Sn}$ . The (Gaussian centroid) energy of the GMR in  $^{116}\text{Sn}$  [18] is  $830 \pm 160$  keV higher than in  $^{116}\text{Cd}$ , whereas the parameterizations in Refs [15–17] lead to predictions of difference from 100–300 keV, much less than the experimental value. The results suggest that the GMR in the Cd isotopes are abnormally low compared to the close shell nuclei of similar mass.

The energy difference between the two Cd isotopes and between the two Sn isotopes are much better determined than the actual energy, as systematic errors (such as strength errors at around 10 MeV due to background, detector threshold effects, continuum choices) should be similar for these nuclei. The difference might be expected to depend mostly on the symmetry term ( $N - Z/A$ ) in the leptodermous expansion, and that is the largest contribution. The right lower panel in Fig. 3 compares calculations for the energy difference between the GMR's in  $^{112}\text{Sn}$  and  $^{124}\text{Sn}$  using the parameterization in Refs [15–17] with the experimental difference, while the left lower panel in Fig. 3 shows the same between the GMR's in  $^{110}\text{Cd}$  and  $^{116}\text{Cd}$ . Except for the S3 interaction ( $K_{nm}=333$  MeV), each of the nonrelativistic interactions used by Nayak *et al.* results in an energy difference much lower than the experimental results. Of the energy difference calculated with the relativistic interactions, only that for NL-C ( $K_{nm} = 224.6$  MeV) falls in the experimental range. The results from the modified Skyrme interactions with  $K_{nm} = 220$  MeV and 240 MeV are consistent with the data, while that for SkK200 is just outside the experimental range. These results are consistent between the Cd isotopes and the Sn isotopes as shown in Fig. 3.

## 5. Conclusions

Most of the expected isoscalar E0 strength in  $^{110}\text{Cd}$ ,  $^{116}\text{Cd}$ ,  $^{112}\text{Sn}$  and  $^{124}\text{Sn}$  has been identified. Predictions using relativistic and nonrelativistic (Skyrme or Skyrme-like) interactions with  $K_{nm} \sim 211\text{--}216$  MeV result in energies slightly above the experimental energies. The energy difference between the E0 position in  $^{112}\text{Sn}$  and  $^{124}\text{Sn}$ , and between  $^{110}\text{Cd}$  and  $^{116}\text{Cd}$  are consistent with relativistic calculations for NL-C parameterization ( $K_{nm} = 224.5$  MeV) and with calculations using modified Skyrme interactions differing from Skyrme primarily in the behavior of the density dependence to provide a more reliable extrapolation to neutron-rich systems.

This work was supported in part by the U.S. Department of Energy under Grant No. DE-FG03-93ER40773 and by The Robert A. Welch Foundation.

## REFERENCES

- [1] J.P. Blaizot, *Phys. Rep.* **64**, 171 (1980).
- [2] S. Stringari, *Phys. Lett.* **108B**, 232 (1982).
- [3] M.M. Sharma, W.T. A. Borghols, S. Brandenburg, S. Crona, A. van der Woude, M.N. Harakeh, *Phys. Rev.* **C38**, 2562 (1988).
- [4] D.H. Youngblood, P. Bogucki, J.D. Bronson, U. Garg, Y.-W. Lui, C.M. Rozsa, *Phys. Rev.* **C23**, 1997 (1981); Y.-W. Lui, P. Bogucki, J.D. Bronson, D.H. Youngblood, U. Garg, *Phys. Rev.* **30**, 51 (1984).
- [5] D.H. Youngblood, Y.-W. Lui, H. L. Clark, *Phys. Rev.* **C65**, 034302 (2002); *Phys. Rev.* **63**, 067301 (2001); *Phys. Rev.* **60**, 014304 (1999).
- [6] K. van der Borg, M.N. Harakeh, A. van der Woude, *Nucl. Phys.* **A365**, 243 (1981).
- [7] H.L. Clark, Y.-W. Lui, D. H. Youngblood, *Phys. Rev.* **C57**, 2887 (1998).
- [8] G.R. Satchler, D. T. Khoa, *Phys. Rev.* **C55**, 285 (1997).
- [9] G. Fricke, C Bernhardt, K. Heilig, L. A. Schaller, L. Schellenberg, E. B. Shera, C. W. DeJager, *At. Data Nucl. Data Tables* **60**, 177 (1995).
- [10] M.N. Harakeh, A. E. L. Dieperink, *Phys. Rev.* **C23**, 2329 (1981).
- [11] S.S. Dietrich, B. L. Berman, *At. Data Nucl. Data Tables* **38**, 199 (1988).
- [12] D.H. Youngblood, Y.-W. Lui, H. L. Clark, B John, Y. Tokimoto, X. Chen, *Phys. Rev.* **C69**, 034315 (2004).
- [13] M. Buenerd, in Proceeding of International Symposium on Highly Excited States and Nuclear Structure, Orsay, France, edited by N. Marty, N. van Giai, (1983).
- [14] G. Duhamel, M. Buenerd, P. de Saintignon, J. Chauvin, D. Lebrun, Ph. Martin, G. Perrin, *Phys. Rev.* **C38**, 2509 (1988).
- [15] R.C. Nayak, J.M. Pearson, M. Farine, P. Gleissl, M. Brack, *Nucl. Phys.* **A516**, 62 (1990).
- [16] M. Farine, J.M. Pearson, F. Tondeur, *Nucl. Phys.* **A615**, 135 (1997).
- [17] T.V. Chossy, W. Stocker, *Phys. Rev.* **C56**, 2518 (1997).
- [18] D.H. Youngblood, H.L. Clark, Y.-W. Lui, *Phys. Rev. Lett.* **82**, 691 (1999)